UNIVERSITY OF CALIFORNIA,
IRVINE

Plastic deformation mechanisms in bimodal structured metals

THESIS

submitted in partial satisfaction of the requirements
for the degree of

MASTER OF SCIENCE

in Material Science and Engineering

by

Han Wang

Thesis Committee:
Assistant Professor Penghui Cao, Chair
Associate Professor Tim Rupert
Assistant Professor William Bowman

2021

DEDICATION

To

my parents and friends

in recognition of their worth

TABLE OF CONTENTS

LIST OF FIGURES

ACKNOWLEDGEMENTS

I would like to express the deepest appreciation to my committee chair, Professor Penghui Cao Irvine, who has the attitude and the substance of a genius and induced me to the world of Molecular Dynamics simulation. Without his help, the thesis would never have the chance to be finished.

I would like to thank my committee members, Professor Tim Rupert and Professor William Bowman, whose work demonstrated to me the beauty of computational and experimental research.

In addition, a thank you to all my friends for the meaningful discussions and to the staffs work at Starbuck and Boba shops that always prepare good drinks that helps me gain energy.

ABSTRACT OF THE THESIS

Plastic deformation mechanisms in bimodal structured metals

by

Han Wang

Master of Science in Material Science and Engineering

University of California, Irvine, 2021

Assistant Professor Penghui Cao, Chair

[An emerging class of heterogeneous nanostructured materials, including bimodal, gradient, hierarchical structures, has attracted increasing attention due to the extraordinary mechanical behaviors such as ultrahigh strength and better tensile ductility, when compared with their homogeneous counterparts. This suggests that the structural heterogeneity intentionally engineered into the materials is essential to promote hardening mechanisms and improve the uniform tensile strain. In this thesis, we focus on plastic deformation and its associated mechanisms in bimodal nanostructured metals. By varying the size of small grain in bimodal structure, we find the intragranular plastic deformation is enhanced because of activation and storage of extra dislocations. This dislocation-mediated forest hardening increases the material strength, alleviating the strength softening in the reverse Hall-Petch regime. These findings may be beneficial to designing heterogeneous structured metals with improved ductility-strength synergy.]

INTRODUCTION

Over the years, the new emergent heterogeneous structures[1], such as gradient[2], bimodal[3], multimodal structures[4], have drawn increasing attention together with their unique mechanical properties. Due to their unique grain size distribution, the strength-ductility-trade-off can thereby be alleviated[1]. It not only exhibits great mechanical behaviors but also provides a way of achieving the desired properties by manipulating the structural features[2]. For example, bimodal nanograined (BNG) copper, with coarse grains embedded in ultrafine grains, was first introduced in 2002[3]. Because of its inhomogeneous microstructure, the strain hardening mechanisms, which stabilize the tensile deformation and delay necking instability, are thereby activated, leading to high strength and ductility, 65% elongation to failure and 30% uniform elongation. Fascinated by the exceptional properties, the bimodal structure was found applicable to other metals, such as nickel[4], aluminum[5], and titanium[6]. All the nanograined metals with bimodal structures obtained superior mechanical properties than their homogeneous nanograined (HNG) counterparts. These experimental studies are suggesting that the grain size ratio between small and large grains plays an extremely fundamental role in the mechanical behavior of bimodal[7][3]. However, the most intrinsic underlying mechanisms of the bimodal structure are still not well understood.

Here, we perform massively parallel atomistic simulations of deformation of BNG Cu with varying grain size ratios and then compare the results with HNG Cu, a material that has been well studied in both experiments and simulations[3][8][9]. It is shown that, with the decreasing small grain size, the strength of large grains is enhanced. Thus, it leads to the

alleviation of the strength softening effect on BNG Cu. This is interesting because it is known that, with the decreasing grain size, the strength of polycrystalline metals will increase first, and after a critical threshold value, it will then experience a drastic downfall[10]. This strength softening effect due to the continuously decreasing grain size is called the inverse Hall-Petch effect[11]. The strength softening in the inverse regime it is governed by grain boundary activities such as stress-induced intergranular sliding[12], dislocation-grain boundary interaction[13], and shear-coupled boundary migration[14][15]. By analyzing the deformation process in our bimodal structure, it is found that with the decreasing size of the grains around the large grains, more dislocations are activated within the large grains. Furthermore, we observe a reduced intergranular grain boundary sliding and migration among large grains. The structural heterogeneity triggers multiple dislocation slip systems, twinning, and the formation of stacking faults, indicating improved plasticity of large grains. The study reveals the underlying deformation mechanisms of heterogeneous structures, which might guide the design of BNG metals.

Chapter 1 Background

Hetero-structured metals are the emerging material research topic. Due to the unique heterogeneity of the grain size distribution, structures such as bimodal structure, gradient structure and lamella structure tend to exhibit superior mechanical and physical properties, especially towards the strength-ductility synergy, that are not attainable by conventional homo-structured metals .

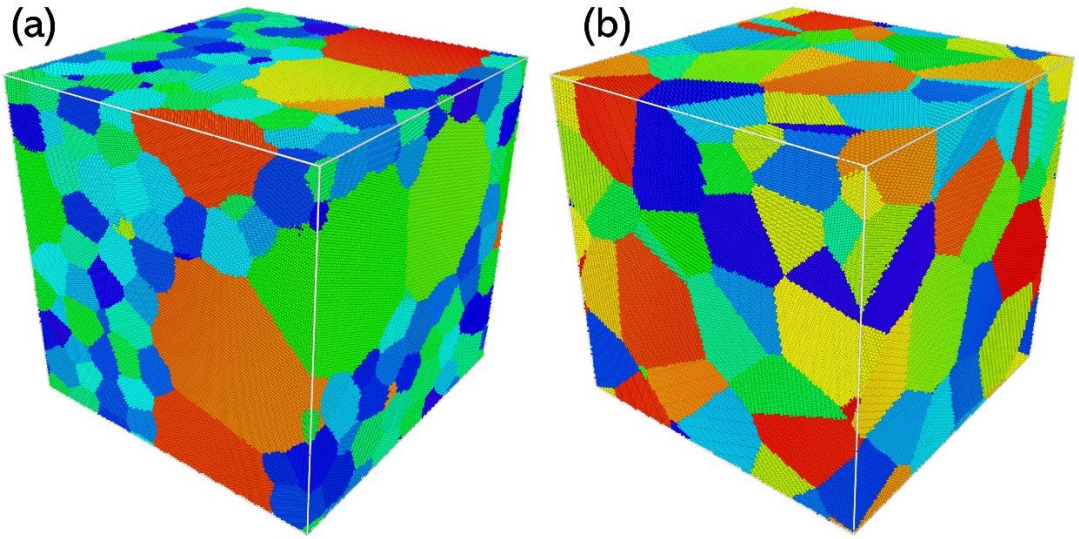

Figure 1.1 | Comparison of bimodal and homogenous structures. (a) A bimodal grained structure with 50 vol% grains of size of 14 mm and 50 vol% grains of 6 mm. (b) A grained structure with random size distribution. The grain is colored according to its orientation assigned randomly.

In 2002, a thermomechanical treatment of Cu that results in a bimodal grain size distribution, with micrometer-sized grains embedded inside a matrix of nanocrystalline and ultrafine (<300 nm) grain, was introduced[3]. The process starts by rolling Cu at liquid nitrogen temperature to a high value of percentage cold work and then annealing. Rolling at liquid nitrogen can suppress dynamic recovery of the grains and achieve the ultrafine grain matrix, and annealing allows the recovery of micrometer-sized grains, together forming a

bimodal grain size distribution. The inhomogeneous microstructure induces strain hardening mechanisms that stabilize the tensile deformation, leading to a high tensile ductility, 65% elongation to failure, and 30% uniform elongation. Bimodal copper can also be produced by equal channel angular pressing (ECAP) followed by annealing at 125°C or, respectively, at 140°C subsequent to the ECAP-process[8]. After the systematic study of the deformation mechanisms and strain rate sensitivity, it was concluded that the bimodality is the deterministic factor of the dominant deformation mechanism and the strain-rate sensitivity. In the ultrafine grain, thermally activated annihilation of dislocation at the grain boundaries govern the mechanical behavior. However, for the coarse grain, the annihilation of dislocation at the interface of coarsened grains to the surrounding ultrafine-grained matrix dominated the mechanical behavior. In addition, the plastic strain recovery deformation behavior was reported in bulk nanocrystalline-ultrafine aluminum[16]. Spark plasma sintering at 620°C is applied to produce the bimodal nano-crystalline-ultrafine Al from consolidation of nanostructured powders, and then it was investigated under in situ compressive loading using high-energy synchrotron X-ray diffraction. After one loading-unloading cycle, to 2% strain, it is found that the reversible peak is hereby broadened within the nanocrystalline grain volume and that tensile residual stress reached 80 MPa within the ultrafine grain volume. Upon unloading, they also discovered recovery of 12% of the plastic strain. With the higher applied deformations to 4%, the recovery would increase up to 28%. The residual stresses induced by the inhomogeneous strains act as a driving force to drive dislocations back to the grain boundaries where they originated.

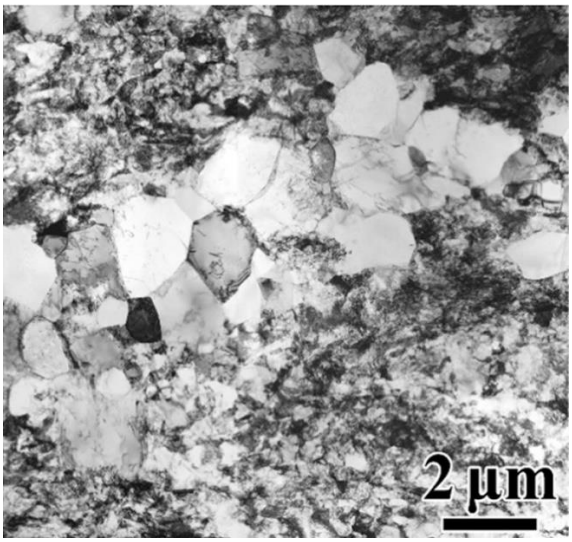

Figure 1.2 | TEM image of Ti with heterogeneous lamella structure, showing a lamella of recrystallized grains in between two lamellae of ultra-fine grains.[17]

Knowing how the heterogeneity can attribute the unusual mechanical behavior, more heterogeneric structured metals were then reported. A heterogeneous lamella structure in Ti produced by asymmetric rolling and partial recrystallization was proved to alleviate the strength and ductility trade-off[17]. It is also found that the unusual high strength is obtained with the assistance of high back stress developed from heterogeneous yielding, whereas the high ductility is attributed to back-stress hardening and dislocation hardening. In addition, a novel process to obtain lamella structured low-carbon steel with bimodal grain size distribution and its corresponding mechanical property was studied[18]. By applying a two-step warm rolling and subsequently annealing the desired structure is then successfully produced, of which the yield strength and tensile strength are increased by 87.4% and 35% respectively when compared with initial coarse grain steel. It is concluded that the enhanced strength mainly comes from the ultrafine grain strengthening, and the reasonable ductility can be attributed to both the bimodal grain size and the lamellar structure, which can

increase the work hardening rate by the accumulation of geometrically necessary dislocations in their vicinity.

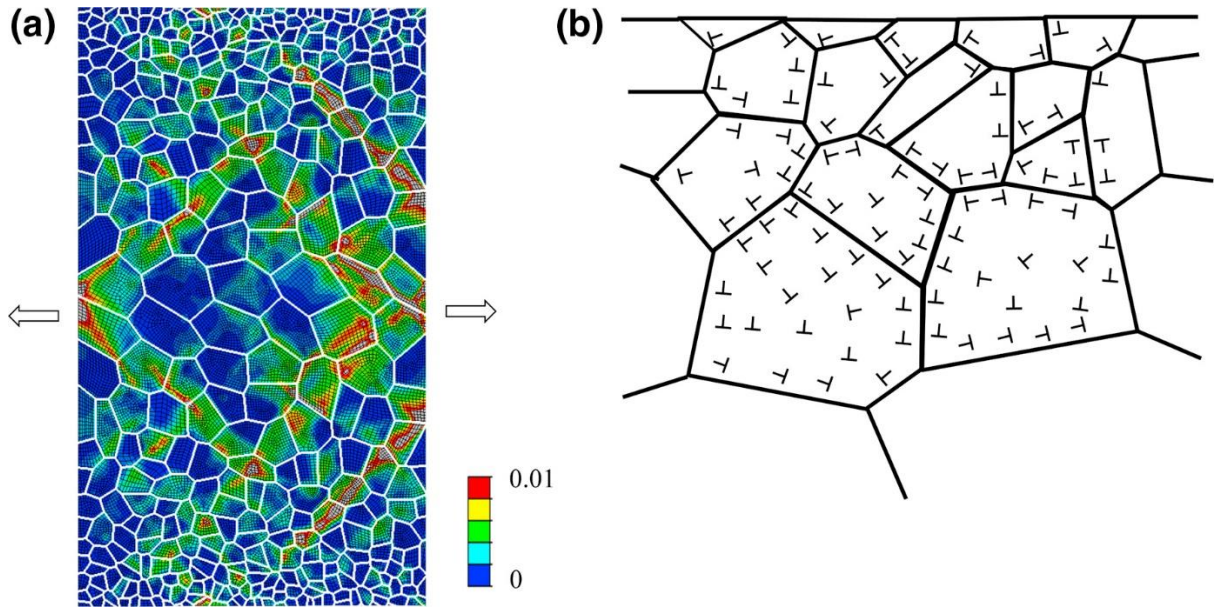

Figure 1.3 | Modeling of plastic strain gradients imposed by gradient nano-grains in Cu. (a) A finite element crystal plasticity model of the quasi-two-dimensional structure of columnar nano-grains was constructed with a continuous spatial gradient of grain sizes linearly varying from ~20 nm in the top/bottom surface layer to ~110 nm in the central region. The sample is pulled under axial tension along the horizontal direction and color by the plastic strains. (b) Schematic illustration of a gradient variation of the density of geometrically necessary dislocations in a gradient nanograined structure.[19]

Besides bimodal and lamella structured metals, nanomaterials with gradient structure, in which the grain size increases from nanoscale at the surface to coarse-grained in the core, also can lead to outstanding mechanical properties. By applying surface plastic deformation onto a bulk coarse-grained metal, the distinctive gradient microstructure was generated from the strain gradient[20]. The extraordinary tensile ductility of the gradient nanograined surface layer, which is several times stronger than the coarse-grained structure, leads to a strength-ductility synergy. In addition, by conducting a surface mechanical grinding treatment (SMGT), a nanograined (NG) Cu film with a spatial gradient in grain size was prepared [21], which achieved large tensile plasticity and revealed a

different governing deformation mechanism. It is concluded that a mechanically driven grain boundary migration process with a substantial concomitant grain growth dominated plastic deformation of the gradient NG structure.

Unlike the conventional mechanical testing methods that are not able to trace the structure changes with respect to the deformation process, Molecular Dynamics (MD) Simulation has become a very efficient way to study the deformation behavior and mechanical properties. By performing massively parallel atomistic simulations in gradient nanograined Cu and homogeneous nanograined Cu[2], it is found that the strongest size, which lies between the Hall-Petch effect and inverse Hall-Petch effect, can be tuned by tailoring grain size gradient, and raising in the gradient shifts in the size toward the smaller value. In addition, the essential deformation mechanisms were also analyzed in this study. The results show that the decrease of strongest size is mainly induced by mitigation of grain boundary-mediated softening and processes together with the enhanced intragranular plastic deformation. The gradient mechanical behavior in gradient nano-grain copper was also studied by a crystal plasticity finite element model[19]. It's revealed that both gradient stress and gradient plastic strain in the cross-section of GNC copper subjected to axial tension. These spatial gradients are from the progressive yielding of the gradient grains under an overall uniform deformation.

In conclusion, the new emergent heterogeneous structures, such as gradient, bimodal, multimodal structures, have drawn attention together with their unique mechanical properties. Due to their unprecedented grain size distribution, the famous strength-ductility-trade-off can thereby be alleviated. It not only exhibits great mechanical behaviors but also provides a way of achieving the desired properties by manipulating the

parameters of structure. However, the most intrinsic underlying deformation mechanisms of the heterogeneous structure are still not well understood, especially lack of support from computation method for bimodal structured metals. As a result, in this study, we performed massively parallel atomistic simulations in bimodal structured metal and revealed its deformation mechanisms.

Chapter 2 Deformation Behavior of Bimodal Structured Metal

In this chapter, the detailed study regarding bimodal structured metal will be introduced, including simulation modal, method, simulation results and conclusions.

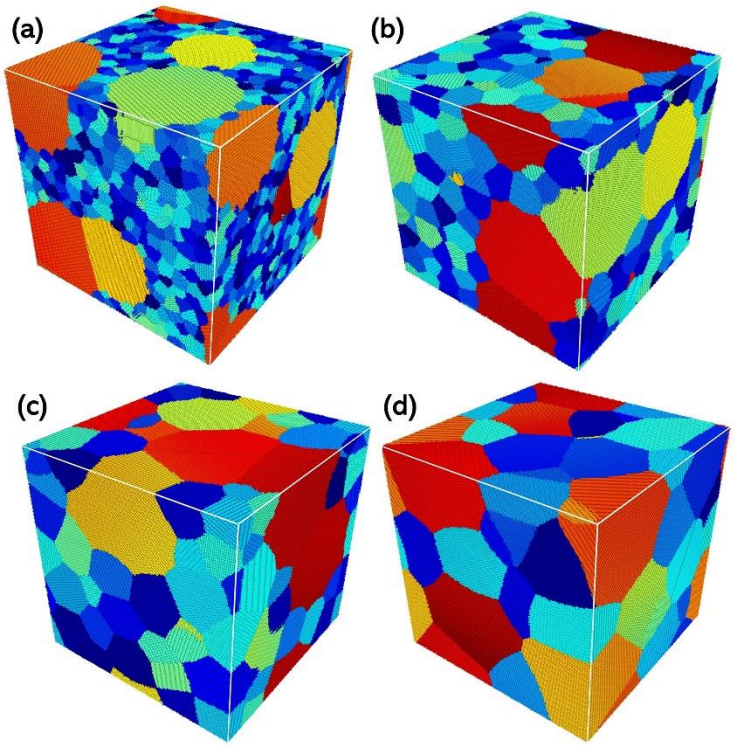

Figure 2.1 | Atomic models of bimodal structured Cu with varying small grain sizes. (a) 3 nm, (b) 6 nm, (c) 10 nm, and (d) 14 nm.

1. Simulation model

The bimodal nanograined structures (BNG) with a box size of 40 nm × 40 nm × 40 nm were generated with Dream.3D[22], which is a 3D structure builder that allows users to construct customized workflows to build synthetic microstructures. To study BNG small grain size *d* effect, the size of the large grain is fixed to 20 nm with the small grain size ranging from 2 nm to 15 nm, and both large grains and small grains take 50% of the structure volume. There are approximately 5.5×10^6 atoms in each BNG, 7650 grains in the BNG with the smallest small grain size, and 27 grains in the BNG with the largest small gain size. A series

of homogeneous structures with the same box size and varying grain sizes are also generated as a comparison. All the grains are randomly orientated. Figure 2.1 shows the typical Bimodal structured Cu with varying small grain sizes from 3 nm to 14 nm.

2. Method

In this study, we performed massively parallel atomistic simulations in BNG Cu with varying grain size ratios and then compared the results with homogeneous nanograined Cu, a material that has been well studied in both experiments and simulations. For Molecular Dynamics (MD) simulations, which is able to track the dynamic trajectory of atoms, the small gains, and the large grains were set as two different atom groups to analyze the mechanical behaviors individually. An embedded-atom method (EAM) potential[23] was set as the interatomic interaction of Cu atoms, and all the simulations were conducted at a constant 300 K using Nosé-Hoover thermo-stat[24][25]. The boundary conditions along *x*, *y*, and *z* directions are all periodic. The structures were first annealed at 300 K, and then a uniaxial tensile strain was applied to the *y* direction. The components of the kinetic energy tensor and the virial tensor from pairwise interaction were considered during the calculations of stress. All samples are deformed at a constant strain rate of 5×10^8 s^{-1}, and the stress in other directions perpendicular to tensile deformation was controlled at zero stress using Berendsen barostat[26]. Later on, different strain rates from 5×10^7 s^{-1} to 1×10^{10} s^{-1} were performed on the BNG with 14 nm small grain size and 20 nm HNG to study the strain rate effect under the same condition.

3. Simulation Results

Figure2.2a shows the normalized flow stress that indicates the softening rate of BNG structures, compared with that of HNG structures. As is illustrated, the softening rate of HNG

structures is decreasing more severely than that of HNG structures, suggesting that the strength softening is suppressed in BNG structures. The calculated average plastic flow stresses from 10% to 20% applied strain for each BNG structure are shown in the inset of Figure 2.2a. With the decreasing small grain size d in BNG, the flow stress is enhanced at first reaching the strongest size at d=14 nm and then experiencing a mild softening with the continuous decrease of d. The flow stresses for large grains and small grains in BNG structures are shown in Figure 2.2b.

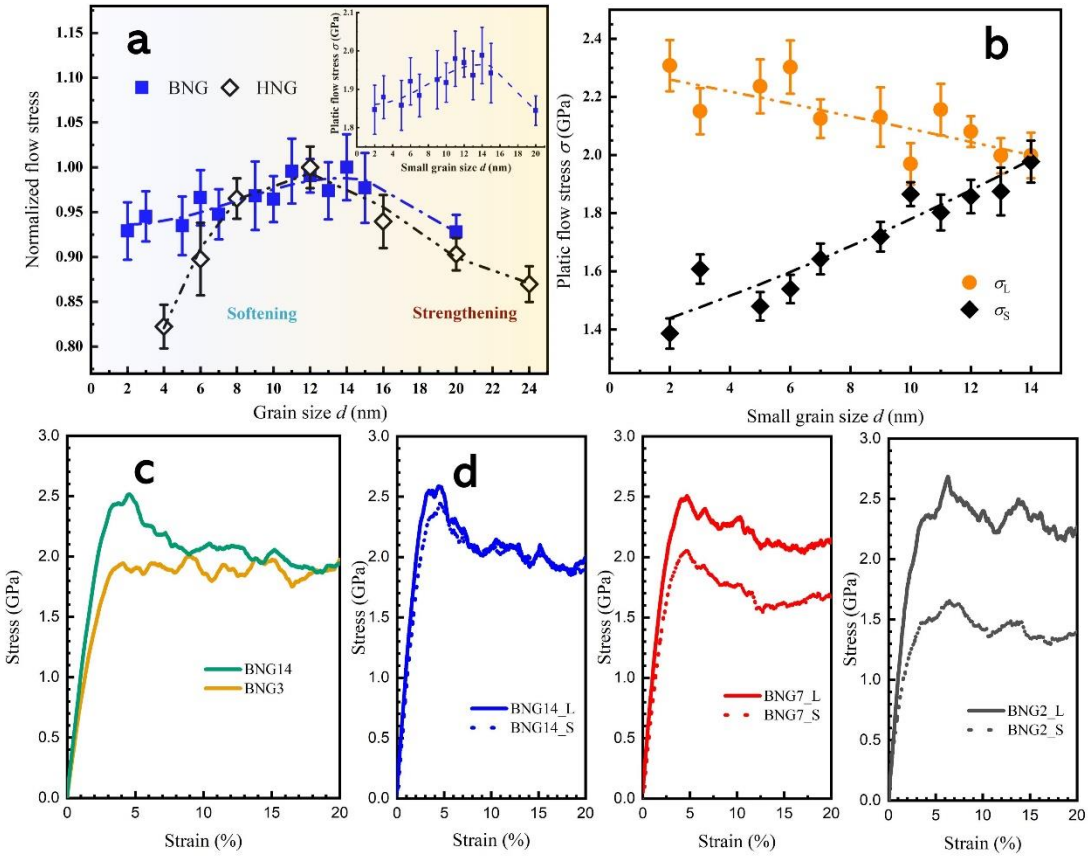

Figure 2.2 | Mechanical properties of bimodal structured Cu. (a) the strength softening rate of BNG structures compared with HNG structures. The inset of (a) is the calculated average plastic flow stress from 10 % to 20 % for BNG and HNG structures. (b) the corresponding plastic flow stresses of large and small grains in BNG structures, respectively. The strain-stress curves of (c) BNG structures with a small grain size of 3 nm and 14 nm and of (d) the large and small grains in BNG structures with small grain sizes of 14 nm, 7 nm, and 2 nm respectively.

Due to the grain size effect, the stress in small grains is constantly decreasing with the decrease of *d*. However, it surprisingly shows enhanced stress in large grains. The competing process of decreasing stress in small grains and enhancing stress in large grains is responsible for the mediated softening rate of BNG structures. The strain-stress curves (SSC) for 20 nm HNG and BNGs with small grain sizes of 3 nm and 14 nm are portrayed in Figure 2.2c. It is depicted that the SSCs of BNG14 and HNG20 both exhibit a bump after the elastic regime, whereas the SSC of BNG3 is more flattened. This is because, with the decreasing small grain size, the grain boundaries can better accommodate the plastic deformation, suggesting a transition of mechanism from dislocation mediated plastic deformation to grain boundary mediated plastic deformation[27]. Figure 2.2d shows the SSCs of a small grain and large grain in BNG structures with a small grain size of 14 nm, 7 nm, and 2 nm, respectively. It is obvious that the two curves are deviating from each other with the decrease of d, exhibiting the same trend in Figure 2.2b.

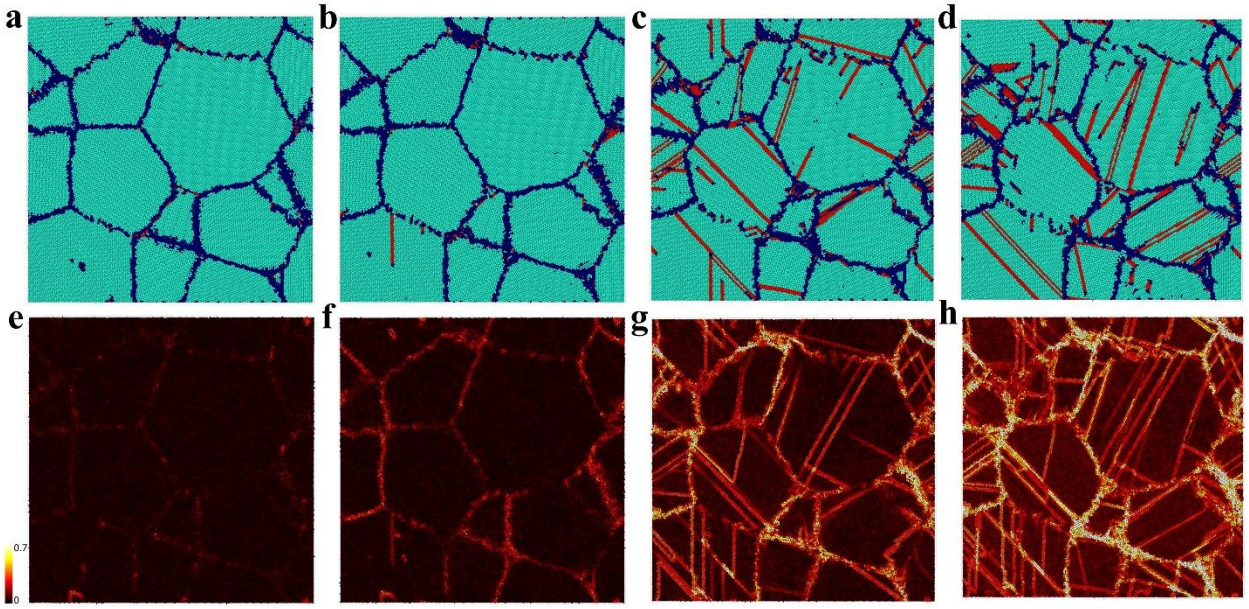

Figure 2.3 | Structure evolution during uniaxial deformation . Deformed BNG structure with small grain size of 14 nm at (a) 1 %, (b) 3 %, (c) 8 %, and (d) 13 % applied strain and the atomic shear strain at (e) 1 %, (f) 3 %, (g) 8 %, and (h) 1 3% applied strain

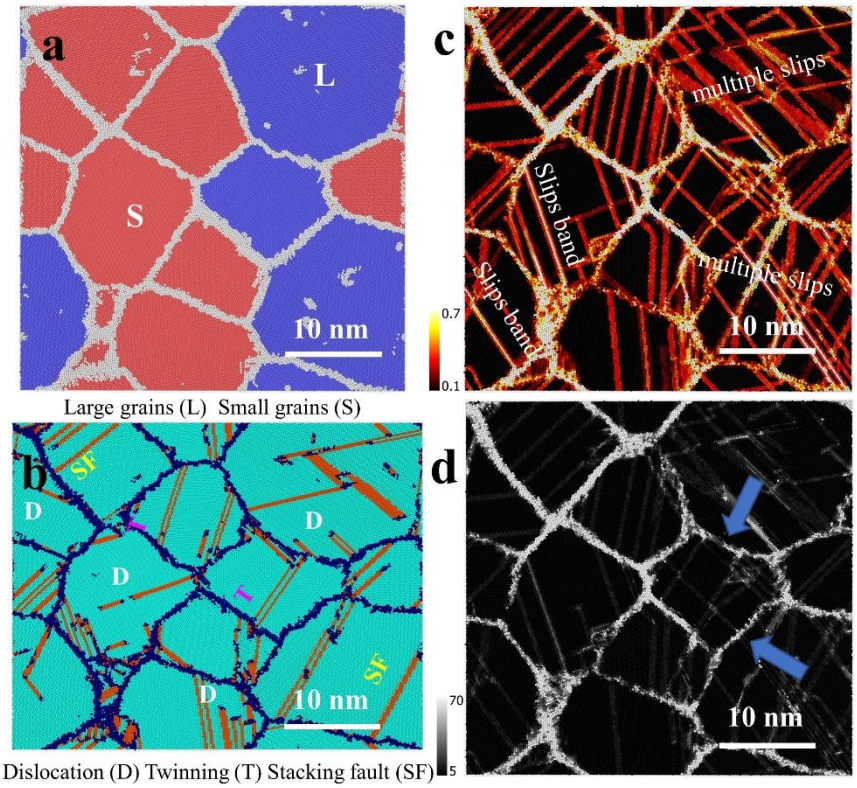

Figure 2.4 | Deformation mechanisms of bimodal structured Cu with a small grain size of 14 nm. (a) the BNG structure with a small grain size of 14 nm after annealing. The deformation mechanisms at 15 % applied strain shown as (b) deformed structure, (c) local atomic shear strain, and (d) the nonaffine squared displacement.

To disclose how the BNG structure evolves while subjected to the applied strain, Figure 2.3 shows the deformed BNG structure with small grain size of 14 nm at 1%, 3%, 8%, and 13% applied strain and its corresponding spatial distribution of atomic shear strain. Upon yielding, dislocations are emitting from the grain boundaries of large grains, as shown in Figure 2.3b, meaning that the large grains will plastically deform first. From Figure 2.3c and 2.3d, it is obvious that after yielding the severe plastic slips accommodates the further deformation and relaxes the whole structure, which leads to the drop of stress shown in Figure 2.2c. However, Figure 2.3a-2.3d are just instantaneous snapshots of the structure; it cannot capture all the ongoing deformation activities. Thus, Figure 2.3e-2.3h illustrates the accumulated slip paths of the structure. As shown in Figure 2.3g and 2.3h, there are more

slips in the large grains, which indicates the plastic deformation can be better accommodated by large grains.

To exemplify the detailed deformation mechanisms underlying the unprecedented strength softening, here we present the schematics of the strongest BNG structures with a small grain size of 14 nm at 15% applied strain, shown by Figure 2.4a-2.4d. Figure 2.4a illustrates the original configuration of the grain distribution after annealing. The blue regime represents the large grains, and the red regime represents the small gains. As shown in Figure 2.4b, deformation mechanisms like dislocation gliding, twinning, and stacking fault are triggered. However, due to the dynamic deformation process, the structures are undergoing drastic defect accumulation and annihilation. Thus, it is unlikely to capture all the ongoing activities within one instantaneous snapshot of the structures. Because of the grain and grain boundary intrinsic heterogeneity, how they accommodate plastic deformation varies accordingly. Unlike dislocation slip, twinning, and stacking fault induced within grains that can be described by linear strain field, grain boundary activities such as grain boundary sliding and migration are more of a nonaffine atomic rearrangement[28][29][30]. As a result, we characterize BNG structures in such a way that

$$\boldsymbol{d}_{ij} = \mathbf{J}_i \boldsymbol{d}_{ij}^0 + \delta \boldsymbol{d}_{ij} \tag{1}$$

where $\boldsymbol{d}_{ij}$ is the distant vector from atom *i* to its neighbor atom *j* in the current state and $\boldsymbol{d}_{ij}^0$ represents the initial state. $\mathbf{J}_i$ is an affine transformation tensor that describes linear deformation like dislocation slip, and $\delta \boldsymbol{d}_{ij}$ captures nonaffine atomic rearrangement. $\mathbf{J}_i$ is obtained by taking the minimum of

$$\boldsymbol{D}_i^2 = \sum_{j=1}^{n_i} \left| \boldsymbol{d}_{ij} - \mathbf{J}_i \boldsymbol{d}_{ij}^0 \right|^2 \quad (2)$$

where n_i is the number of neighboring atoms around atom i. By this, the atomic shear strain η, which captures the plastic slip in the grain interior, can be obtained, and by minimizing $\boldsymbol{D}_i^2$, it can precisely characterize the nonaffine grain boundary activities. Figure 2.4c exhibits the spatial distribution of atomic shear strain η in BNG structure with a small grain size of 14 nm at 15% applied strain. The brighter lines in the grain interior are caused by more than one dislocation gliding through the grain, forming a typical slip band. It is noteworthy that slips in small grains are mostly parallel to each other, whereas there are more cross slips happening in large grains. This means multiple slip systems are triggered in large grains, indicating the domination of dislocation mediated plastic deformation in large grain regimes. The grain boundary activities captured by nonaffine squared displacement $\boldsymbol{D}_i^2$ at the same state as Figure 2.4c is shown in Figure 2.4d. The variations of the white and grey areas exhibit different degrees of grain boundary activity performance. It is depicted that the small grain regime is undergoing severer grain boundary activities compared with the large grain regime (arrows), leading to enhanced plasticity in the large grains.

To study the BNG structures in the inverse Hall-Petch effect regime, the deformation mechanisms of a typical BNG structure with a small grain size of 6 nm are also analyzed in Figure 2.5a-2.5d. Compared with Figure 2.4b, the same deformation qualities are also exhibited in the BNG structure with a small grain size of 6 nm as shown in Figures 2.5b. However, in Figure 2.5d, which maps the spatial distribution of nonaffine squared displacement, the small grain regime does not experience severer grain boundary activities as expected. This identification suggests that the grain boundaries of small grains are

stabilized by the unique bimodal grain size distribution, which might explain the alleviation of the strength softening rate.

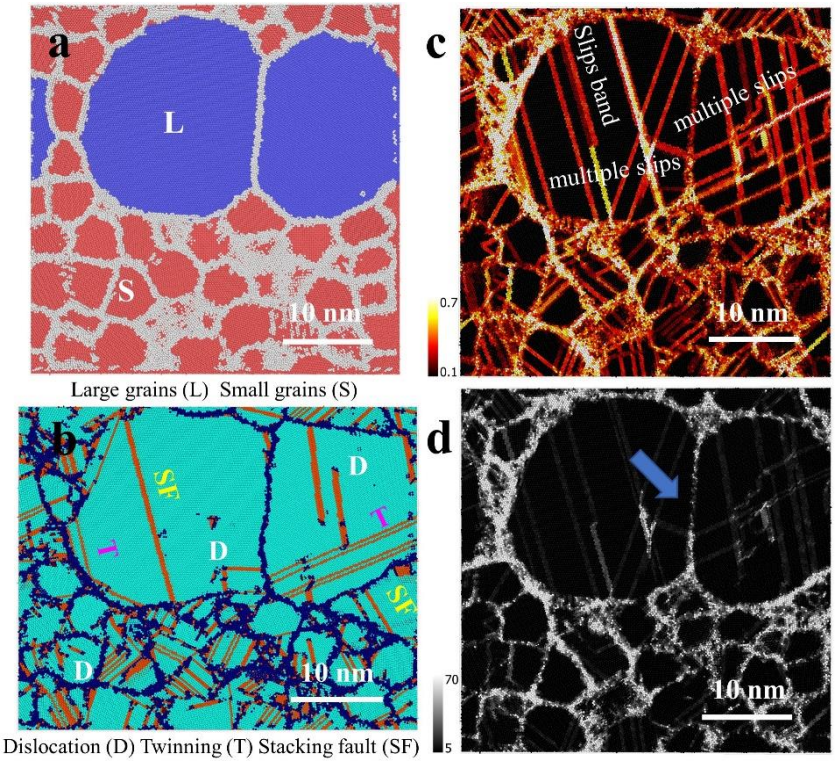

Figure 2.5 | Deformation mechanisms of bimodal structured Cu with a small grain size of 6 nm. (a) the BNG structure with a small grain size of 6 nm after annealing. The deformation mechanisms at 15 % applied strain shown as (b) deformed structure, (c) local atomic shear strain, and (d) the nonaffine squared displacement.

To further disclose how the decrease of small grain size *d* affects the plastic slip and grain boundary activities, the atomic shear strain < η > and nonaffine squared displacement < $\boldsymbol{D}^2_{min}$ > are investigated and plotted as a function of small grain size *d* as shown in Figure 2.6a. With the decreasing *d*, after the plain segment the atomic shear strain < η > first increases and then starts to drop when *d* is less than 4 nm. The increasing < η > is induced by the enhanced plasticity in the large grains, which corresponds to the increasing plastic flow stress of large grains in Figure 2.2b. Later on, the increasing < η > of large grains yields to the decreasing < η > of small grains and then causes the drop of overall < η >. On the

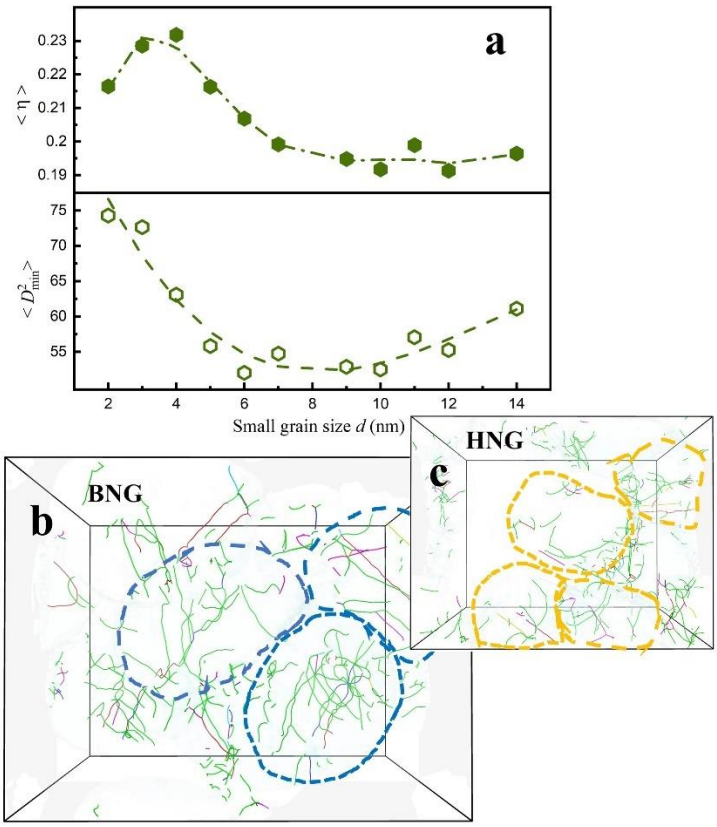

Figure 2.6 | (a) The nonaffine squared displacement $< \boldsymbol{D}^2_{min} >$ and atomic shear strain < η > plotted as a function of small grain size *d* at 15 % applied strain. (b) the dislocation distribution in 20 nm large grains of BNG structure with a small grain size of 2 nm at 20 % applied strain, compared with (d) 20 nm HNG at 20 % applied strain.

contrary, the nonaffine squared displacement $< \boldsymbol{D}^2_{min} >$ first decreases and then starts to increase when the small grains size *d* is less than 6 nm, indicating that with the decrease of small grain size *d*, the grain boundaries are first stabilized, leading to less grain boundary activities, and then yields to the softening effect of the small grains. In a nutshell, while decreasing the small grain size *d* of BNG, the structure will first experience enhanced plasticity and stabilized grain boundaries but then surrender to the softening effect of the small grains with the continuous decreasing of the small grain size *d*. What's more, Figure 2.6b shows the dislocation distribution of the large grains in BNG with a small grain size of 2 nm at 20% applied strain. In order to show a clearer dislocation distribution of large grains, all the small grains are removed, and at least two large grains (blue circles) are exposed

without overlapping with other grains. Figure 2.6c shows the dislocation distribution of HNG (orange circles) with the same grain size as the large grains in Figure 9b at 20% applied strain, and the structure is also modified under the same condition as Figure 9b. From the comparison, it is clear that there is more dislocation generated in the large grains of BNG structure, confirming the enhanced plasticity in large grains, and this also co-relates to the experimental results[8].

Investigation on strain rate changes is one of the critical processes to reveal the deformation mechanisms of metal[31][32], from which the strain rate sensitivity *m* can be calculated and defined by

$$m = \frac{\partial ln\sigma}{\partial ln\dot{\varepsilon}} \tag{2}$$

Figure 2.7a shows the plastic flow stress changes with respect to the variation of strain rate for 20 nm HNG structure and BNG structure with small grain size of 14 nm respectively. By comparing the values of strain rate sensitivity *m*, it is obvious that the BNG structure is less sensitive to strain rate changes than the HNG structure, so that the flow stress drop of the BNG structure is less than that of the HNG structure at the same scale of the strain rate change. However, previous studies have stated that with the decrease of mean grain size, there will be an increase of strain rate sensitivity[31][33]. To elucidate the surprising strain rate sensitivity of BNG, the total lengths of different dislocation types and the percentages of different atom types in the BNG and HNG structures deformed at 5×10^7 s^{-1} are compared in Figure 2.7b, and Figure 2.7c-d illustrate the detailed dislocation distribution in the BNG and HNG structures respectively. As the key dislocation types that govern plastic slip, the total length of Shockley partial dislocation[34] and the total length of

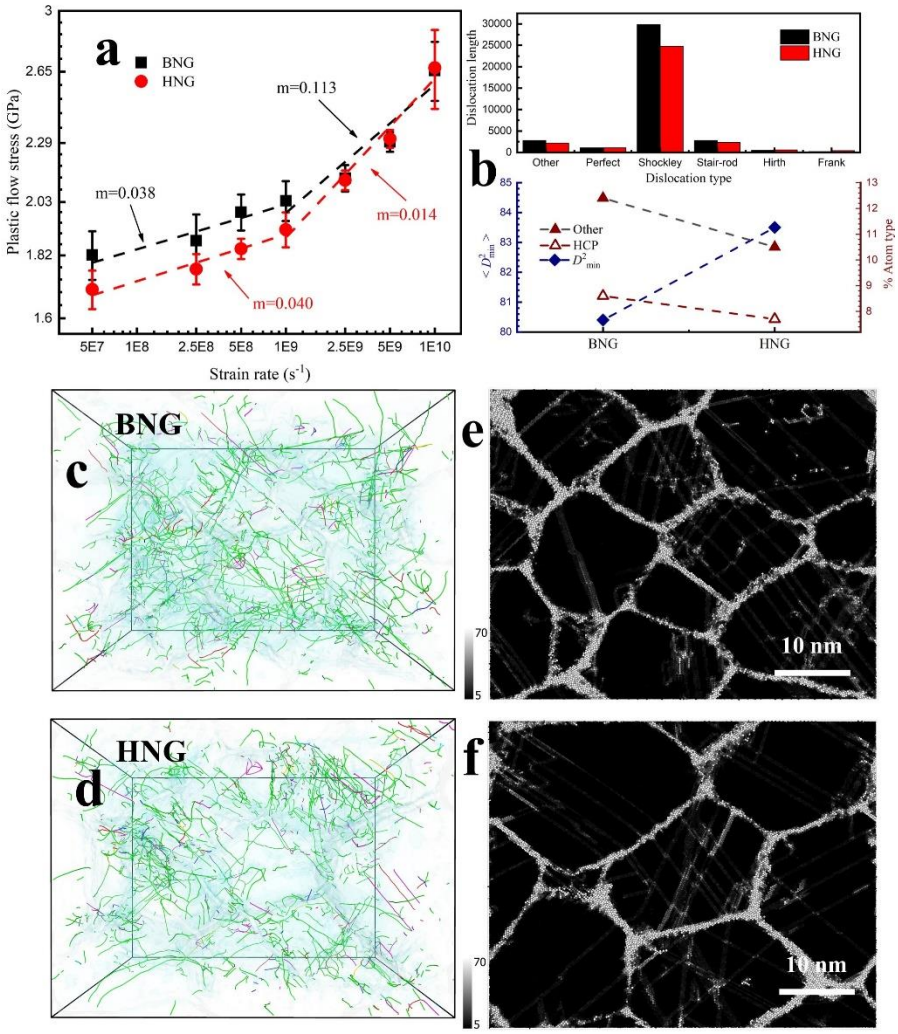

Figure 2.7 | Strain rate effect on BNG Cu. (a) the BNG structure with small grain size of 6 nm after annealing. The deformation mechanisms at 15 % applied strain shown as (b) deformed structure, (c) local atomic shear strain, and (d) the nonaffine squared displacement.

stair-rod dislocation[13], which is formed by two Shockley partial dislocations meeting and blocking each other, are both higher in the BNG structure, which is responsible for the excessive strength of the BNG structure compared with the HNG structure. By analyzing the structure types of each atom, defects such as dislocation, twinning, and stacking fault can be characterized by HCP atom type, and grain boundaries otherwise will be categorized to Other atom type due to the amorphous state. As a result, unlike the HNG structure, the fact that the percentage of HCP atom type is higher in the BNG structure also explains why there

is no sharp drop with even a smaller mean grain size. It is noteworthy that the percentage of Other atom type which represents grain boundary atoms is also higher in BNG , meaning the grain boundaries take a larger portion of volume in the BNG structure compared with that of the HNG structure. Figure 2.7c and 2.7d map the spatial distribution of nonaffine squared displacement $< \boldsymbol{D}_{min}^2 >$ for the BNG and HNG structures respectively. It is obvious that the grain boundaries in the HNG structure are in brighter color than that of the BNG structure, suggesting severer grain boundaries activities. This can also be confirmed by the calculated average $< \boldsymbol{D}_{min}^2 >$ values in Figure 2.7b. As a result, even though grain boundaries take a greater portion of volume in the BNG structure, it is still experiencing less grain boundary activities than the HNG structure, indicating the stabilized grain boundaries and the localized plastic deformation in the large grains by the unprecedented bimodal structure[8].

Chapter 3 Summary and Conclusions

This study manifests the effect of grain size ratio on the mechanical behavior of bimodal nanograined metals. It is found that the alleviated softening rate of BNG in the inverse Hall-Petch regime is induced by the enhanced plasticity of large grains and mitigated intergranular grain boundary activities. Dislocation-mediated deformation mechanisms are believed to contribute the most to the strengthening of nanograined structures[35]. During deformation, dislocation pile-up will be formed at the vicinity of grain boundaries, causing stress concentration at the end of dislocation pile-up. At the same time, a back-stress will be produced pointing to the dislocation source. When the stress concentration at the grain boundary accumulates to the threshold value of triggering the slip system in the neighboring grains, the grain will then yield compromised plasticity. With the decrease of grain size, the grain will be more reluctant to trigger the slip systems in the grains, which is also known as grain boundary strengthening[36]. Thus, the decreasing size of the neighboring grains around the large grains will give rise to the increase of back-stress so that the large grains can accommodate further deformation. It is also suggested that thermally activated annihilation of dislocations at grain boundaries for large grains is the dominating deformation mechanism for the BNG structures, and the additional dislocation can be stored at the grain boundaries in order to keep the compatibility of the material, thus, by which the recovery processes of dislocation at the grain boundaries might also be hindered[8]. Our results on the understanding of mitigated softening rate in inverse Hall-Petch effect regime for the BNG structures shed light on the understanding of the fundamental deformation

mechanisms for emergent heterogeneous structures and guide the improvement of strength-ductility synergy.

Reference

[1] E. Ma and T. Zhu, "Towards strength–ductility synergy through the design of heterogeneous nanostructures in metals," *Mater. Today*, vol. 20, no. 6, pp. 323–331, 2017, doi: 10.1016/j.mattod.2017.02.003.

[2] P. Cao, "The Strongest Size in Gradient Nanograined Metals," *Nano Lett.*, vol. 20, no. 2, pp. 1440–1446, 2020, doi: 10.1021/acs.nanolett.9b05202.

[3] Y. Wang, M. Chen, F. Zhou, and E. Ma, "High tensile ductility in a nanostructured metal," *Nature*, vol. 419, no. 6910, pp. 912–915, 2002, doi: 10.1038/nature01133.

[4] Y. Zhao *et al.*, "High tensile ductility and strength in bulk nanostructured nickel," *Adv. Mater.*, vol. 20, no. 16, pp. 3028–3033, 2008, doi: 10.1002/adma.200800214.

[5] N. Tsuji, Y. Ito, Y. Saito, and Y. Minamino, "Strength and ductility of ultrafine grained aluminum and iron produced by ARB and annealing," *Scr. Mater.*, vol. 47, no. 12, pp. 893–899, 2002, doi: 10.1016/S1359-6462(02)00282-8.

[6] X. Wu and Y. Zhu, "Heterogeneous materials: a new class of materials with unprecedented mechanical properties," *Mater. Res. Lett.*, vol. 5, no. 8, pp. 527–532, 2017, doi: 10.1080/21663831.2017.1343208.

[7] Y. Zhao, Y. Zhu, and E. J. Lavernia, "Strategies for improving tensile ductility of bulk nanostructured materials," *Adv. Eng. Mater.*, vol. 12, no. 8, pp. 769–778, 2010, doi: 10.1002/adem.200900335.

[8] J. Bach, M. Stoiber, L. Schindler, H. W. Höppel, and M. Göken, "Deformation mechanisms and strain rate sensitivity of bimodal and ultrafine-grained copper," *Acta Mater.*, vol. 186, pp. 363–373, 2020, doi: 10.1016/j.actamat.2019.12.044.

[9] J. Schiøtz, F. D. Di Tolla, and K. W. Jacobsen, "Softening of nanocrystalline metals at very small grain sizes," *Nature*, vol. 391, no. 6667, pp. 561–563, 1998, doi: 10.1038/35328.

[10] Z. C. Cordero, B. E. Knight, and C. A. Schuh, "Six decades of the Hall–Petch effect – a survey of grain-size strengthening studies on pure metals," *Int. Mater. Rev.*, vol. 61, no. 8, pp. 495–512, 2016, doi: 10.1080/09506608.2016.1191808.

[11] C. E. Carlton and P. J. Ferreira, "What is behind the inverse Hall-Petch effect in nanocrystalline materials?," *Acta Mater.*, vol. 55, no. 11, pp. 3749–3756, Jun. 2007, doi: 10.1016/j.actamat.2007.02.021.

[12] T. J. Rupert, D. S. Gianola, Y. Gan, and K. J. Hemker, "Experimental observations of stress-driven grain boundary migration," *Science (80-.).*, vol. 326, no. 5960, pp. 1686–1690, 2009, doi: 10.1126/science.1178226.

[13] V. Yamakov, D. Wolf, S. R. Phillpot, and H. Gleiter, "Dislocation-dislocation and dislocation-twin reactions in nanocrystalline Al by molecular dynamics simulation," *Acta Mater.*, vol. 51, no. 14, pp. 4135–4147, 2003, doi: 10.1016/S1359-

6454(03)00232-5.

[14] A. Rajabzadeh, F. Mompiou, M. Legros, and N. Combe, "Elementary mechanisms of shear-coupled grain boundary migration," *Phys. Rev. Lett.*, vol. 110, no. 26, pp. 1–5, 2013, doi: 10.1103/PhysRevLett.110.265507.

[15] S. L. Thomas, K. Chen, J. Han, P. K. Purohit, and D. J. Srolovitz, "Reconciling grain growth and shear-coupled grain boundary migration," *Nat. Commun.*, vol. 8, no. 1, pp. 1–12, 2017, doi: 10.1038/s41467-017-01889-3.

[16] I. Lonardelli, J. Almer, G. Ischia, C. Menapace, and A. Molinari, "Deformation behavior in bulk nanocrystalline-ultrafine aluminum: in situ evidence of plastic strain recovery," *Scr. Mater.*, vol. 60, no. 7, pp. 520–523, 2009, doi: 10.1016/j.scriptamat.2008.11.045.

[17] X. Wu *et al.*, "Heterogeneous lamella structure unites ultrafine-grain strength with coarse-grain ductility," *Proc. Natl. Acad. Sci. U. S. A.*, vol. 112, no. 47, pp. 14501–14505, 2015, doi: 10.1073/pnas.1517193112.

[18] J. Sun *et al.*, "A novel process to obtain lamella structured low-carbon steel with bimodal grain size distribution for potentially improving mechanical property," *Mater. Sci. Eng. A*, vol. 785, no. March, p. 139339, 2020, doi: 10.1016/j.msea.2020.139339.

[19] Z. Zeng, X. Li, D. Xu, L. Lu, H. Gao, and T. Zhu, "Gradient plasticity in gradient nano-grained metals," *Extrem. Mech. Lett.*, vol. 8, pp. 213–219, 2016, doi: 10.1016/j.eml.2015.12.005.

[20] L. Ke, "Making strong nanomaterials ductile with gradients," *Science (80-.).*, vol. 345, no. 6203, pp. 1455 LP – 1456, 2014.

[21] N. Copper, T. H. Fang, W. L. Li, N. R. Tao, and K. Lu, "Tensile Plasticity in Gradient," *Science (80-.).*, vol. 331, no. March, pp. 1587–1590, 2011.

[22] M. A. Groeber and M. A. Jackson, "Groeber and Jackson Integrating Materials and Manufacturing Innovation," vol. 3, p. 5, 2014.

[23] S. M. Foiles, M. I. Baskes, and M. S. Daw, "Embedded-atom-method functions for the fcc metals Cu, Ag, Au, Ni, Pd, Pt, and their alloys," *Phys. Rev. B*, vol. 33, no. 12, pp. 7983–7991, 1986, doi: 10.1103/PhysRevB.33.7983.

[24] S. Nosé, "A molecular dynamics method for simulations in the canonical ensemble," *Mol. Phys.*, vol. 52, no. 2, pp. 255–268, 1984, doi: 10.1080/00268978400101201.

[25] W. G.Hoover, "Canonical dynamics: Equilibrium phase-space distributions," *Phys. Rev. A*, vol. 31, no. 1695, 1985, doi: 10.1007/BF00419952.

[26] H. J. C. Berendsen, J. P. M. Postma, W. F. Van Gunsteren, A. Dinola, and J. R. Haak, "Molecular dynamics with coupling to an external bath," *J. Chem. Phys.*, vol. 81, no. 8, pp. 3684–3690, 1984, doi: 10.1063/1.448118.

[27] J. Hu, Y. N. Shi, X. Sauvage, G. Sha, and K. Lu, "Grain boundary stability governs

hardening and softening in extremely fine nanograined metals," *Science (80-.).*, vol. 355, no. 6331, pp. 1292–1296, 2017, doi: 10.1126/science.aal5166.

[28] F. Shimizu, S. Ogata, and J. Li, "Theory of shear banding in metallic glasses and molecular dynamics calculations," *Mater. Trans.*, vol. 48, no. 11, pp. 2923–2927, 2007, doi: 10.2320/matertrans.MJ200769.

[29] C. C. Wang *et al.*, "Real-time, high-Resolution study of nanocrystallization and fatigue cracking in a cyclically strained metallic glass," *Proc. Natl. Acad. Sci. U. S. A.*, vol. 110, no. 49, pp. 19725–19730, 2013, doi: 10.1073/pnas.1320235110.

[30] P. Cao, M. P. Short, and S. Yip, "Understanding the mechanisms of amorphous creep through molecular simulation," *Proc. Natl. Acad. Sci. U. S. A.*, vol. 114, no. 52, pp. 13631–13636, 2017, doi: 10.1073/pnas.1708618114.

[31] Q. Wei, S. Cheng, K. T. Ramesh, and E. Ma, "Effect of nanocrystalline and ultrafine grain sizes on the strain rate sensitivity and activation volume: Fcc versus bcc metals," *Mater. Sci. Eng. A*, vol. 381, no. 1–2, pp. 71–79, 2004, doi: 10.1016/j.msea.2004.03.064.

[32] T. Zhang, K. Zhou, and Z. Q. Chen, "Strain rate effect on plastic deformation of nanocrystalline copper investigated by molecular dynamics," *Mater. Sci. Eng. A*, vol. 648, pp. 23–30, 2015, doi: 10.1016/j.msea.2015.09.035.

[33] J. Chen, L. Lu, and K. Lu, "Hardness and strain rate sensitivity of nanocrystalline Cu," *Scr. Mater.*, vol. 54, no. 11, pp. 1913–1918, 2006, doi: 10.1016/j.scriptamat.2006.02.022.

[34] J. Wang and H. Huang, "Shockley partial dislocations to twin: Another formation mechanism and generic driving force," *Appl. Phys. Lett.*, vol. 85, no. 24, pp. 5983–5985, 2004, doi: 10.1063/1.1835549.

[35] X. Li, Y. Wei, W. Yang, and H. Gao, "Competing grain-boundary- and dislocation-mediated mechanisms in plastic strain recovery in nanocrystalline aluminum," *Proc. Natl. Acad. Sci. U. S. A.*, vol. 106, no. 38, pp. 16108–16113, 2009, doi: 10.1073/pnas.0901765106.

[36] N. Hansen, "Hall-petch relation and boundary strengthening," *Scr. Mater.*, vol. 51, no. 8 SPEC. ISS., pp. 801–806, 2004, doi: 10.1016/j.scriptamat.2004.06.002.